Original Article
AAL exacerbates pro-inflammatory response in macrophages by regulating Mincle/Syk/Card9 signaling along with the Nlrp3 inflammasome assembly

Zhijun Zhang[1], Long He[1], Shuang Hu[1], Yi Wang[1], Qiaohong Lai[1], Ping Yang[1], Qilin Yu[1], Shu Zhang[1], Fei Xiong[1], Sakine Simsekyilmaz[1], Qin Ning[2], Jinxiu Li[3], Dongshan Zhang[3], Hongliang Zhang[3], Xudong Xiang[3], Zhiguang Zhou[4], Hui Sun[5], Cong-Yi Wang[1]

[1]The Center for Biomedical Research, [2]Department of Infectious Disease, Institute of Infectious Disease, Tongji Hospital, Tongji Medical College, Huazhong University of Science and Technology, 1095 Jiefang Ave., Wuhan 430030, China; [3]Department of Emergency Medicine, Institute of Emergency Medicine and Rare Diseases, The Second Xiangya Hospital, Central South University, Changsha, China; [4]Diabetes Center, Key Laboratory of Diabetes Immunology, The Second Xiangya Hospital, Central South University, Changsha, China; [5]College of Life Sciences, Wuhan University, Wuhan, China

Abstract: Previously, we demonstrated that Agrocybe aegerita lectin (AAL), a galectin isolated from edible mushroom Agrocybe aegerita, exerts potent anti-tumor activity, while the mechanisms by which AAL suppresses tumor growth are yet to be elucidated. Here, we conducted studies with focus for its impact on the cecal ligation and puncture (CLP)-induced innate immune response. Administration of AAL significantly exacerbated the severity of CLP-induced septic shock as manifested the increased lethality. AAL promoted inflammatory cytokine production by preferentially regulating macrophage activation and recruitment. Mechanistic studies revealed that AAL likely targets macrophages through receptor Mincle to activate Syk/Card9 signaling, which then couples to the Nlrp3 inflammasome assembly. It was further noted that AAL markedly promotes H3K4 di- and trimethylation, by which it enhances Hmgb1 expression. Specifically, AAL induced macrophages secretion of copious amount of Hmgb1 as manifested the Hmgb1 cytoplasmic translocation along with the detection of extracellular Hmgb1. AAL also stimulated a significant increase for nuclear Hmgb1, which then formed a complex with RelA, and thereby enhancing NF-κB transcriptional activity. Together, our data suggest that AAL may possess important pharmaceutical properties in the regulation of innate immune response.

Keywords: AAL, CLP, septic shock, innate immunity, mincle, Nlrp3 inflammasome, methylation, Hmgb1, NF-κB

Introduction

Macrophage plays an important role both in innate and adaptive immune responses. During the course of pro-inflammatory response macrophage may exert dual functions depending on their phenotypes. Particularly, M1 macrophage serves as a potent mediator for the initiation and progression of inflammatory response by producing large amounts of pro-inflammatory cytokines [1, 2], and TNF-α is a typical macrophage-derived Th1 cytokine with potent inflammatory properties [3]. In contrast, M2 macrophage secretes copious amount of Th2 cytokines such as IL-10 to limit the intensity of immune response for prevention of overactive and related tissue or organ damage [4-6].

Agrocybe aegerita lectin (AAL) is isolated from the edible mushroom Agrocybe aegerita, and belongs to the galactose lectin family with a unique carbohydrate recognition domain [7]. Previously, we demonstrated that AAL possesses potent anti-tumor activity in various cancer cells [8, 9]. However, the mechanisms by which AAL suppresses tumor growth are yet to be elucidated. Here, we conducted studies with focus for its impact on the induction of pro-inflammatory response in macrophages by employing a sepsis model induced by cecal ligation and puncture (CLP). In line with its anti-tumor property, administration of AAL promoted CLP-induced lethality. Particularly, AAL stimulates macrophages secretion of copious amount of inflammatory cytokines, while it does not have

a perceptible impact on dendritic cells (DCs). AAL interacts with inducible C-type lectin (Mincle) to activate the Syk/Card9 signaling, which then couples with Nlrp3 inflammasome to induce pro-inflammatory response. Specifically, AAL impacts H3K4 di-/trimethylation to modulate Hmgb1 subcellular location, and by which it activates NF-κB to initiate the transcription of inflammatory cytokines.

Materials and methods

AAL purification

Dry agrocybe aegerita fruiting bodies were crushed into powder and then subjected to AAL purification as previously reported [9]. The purified AAL was dialyzed in PBS overnight and then passed through polymyxin B columns (Sigma, Louis, MO, USA) to remove potentially contaminated endotoxin [10]. The concentration for endotoxin in harvested AAL was < 60 pg/μg protein, and LD50 to mice was 15.85 mg/kg by intraperitoneal injection.

Induction of septic shock

Male C57BL/6 mice (7wk old, 25-30 g) were purchased from the Animal Experimental Center of Hubei province (Wuhan, China). The mice were housed in a specific pathogen-free (SPF) facility with free access to sterile acidified water and irradiated food. After a minimum one week of acclimation, the mice were subjected to CLP induction (see below) along with intraperitoneal administration of AAL (10 mg/kg) or PBS (control vehicle) 12 h before and right after surgery, respectively. Mice undergone sham surgeries were served as controls. All studies were conducted according to the NIH guidelines and approved by the Institutional Animal Care and Use Committee at the Tongji Hospital, Huazhong University of Science and Technology.

Septic shock was induced by cecal-ligation and puncture (CLP) as previously described [11]. Briefly, the mice were anesthetized with pentobarbiturate (80 μg/kg) and the abdomen was opened through a 1-cm incision. The cecum was isolated and ligated with a 4-0 silk suture at 1/2 and punctured at two distinct areas with a 21-gauge needle. After removing the needle, a small amount (droplet) of feces was extruded from both holes. The abdomen was closed in two layers with a 6-0 silk suture. Sham mice were undergone similar surgery processes but

without CLP. In general, 10 mice from each group were employed for monitoring mortality up to 7 days after CLP induction, while additional 5 mice from each group were sacrificed 48 h after CLP to collect heart, liver, lung, kidney, spleen and blood.

Culture of bone marrow-derived macrophages (BMDMs) and RAW 264.7 cells

BMDMs were isolated as previously described with minor modifications [11]. Briefly, bone marrow cells were isolated from femurs of C57BL/6 mice and cultured in the presence of M-CSF (20 ng/ml, eBioscience, San Diego, CA, USA). The supernatant containing non-adherent cells was discarded at day 3 and replaced by fresh media containing M-CSF. Adherent BMDMs were harvested at day 7 for experimental purpose. RAW 264.7 cells and BMDMs were incubated for 12 h with Laminarin (100 μg/ml, an inhibitor for Dectin-1, Sigma, Louis, MO, USA) and/or TJ-M2010-5 (10 μM, an inhibitor for MyD88, provided by Dr. Ping Zhou, Institute of Organ Transplantation, Tongji Hospital) along with AAL (0, 5, 10, 20, 40, 80 μg/ml) in the presence or absence of ATP (4 mM) for 30 min, or incubated with 40 μg/ml AAL as above with different time (0, 2, 6, 12, 24, 48 h), followed by flow cytometry analysis of F4/80$^+$ cells.

Histological analysis

The harvested hearts, livers, lungs and kidneys were fixed in 4% paraformaldehyde, embedded in paraffin and then subjected to histological analysis as reported [12]. Pathological changes in tissue sections (3 sections each mouse, 3 mice each group) were assessed by two pathologists in a blinded fashion at 200× magnification. Inset pictures are shown in 800× magnification.

ELISA

Cytokine levels in the serum and culture supernatant were determined by sandwich ELISA specific for TNF-α, IL-6 and IL-1β using paired capture and detection Abs in ELISA kits (eBioscience, San Diego, CA, USA or BD Biosciences, San Jose, CA, USA) as previously described [13].

Flow cytometry

Single-cell suspensions were prepared from spleens of mice 48 h after CLP as previously
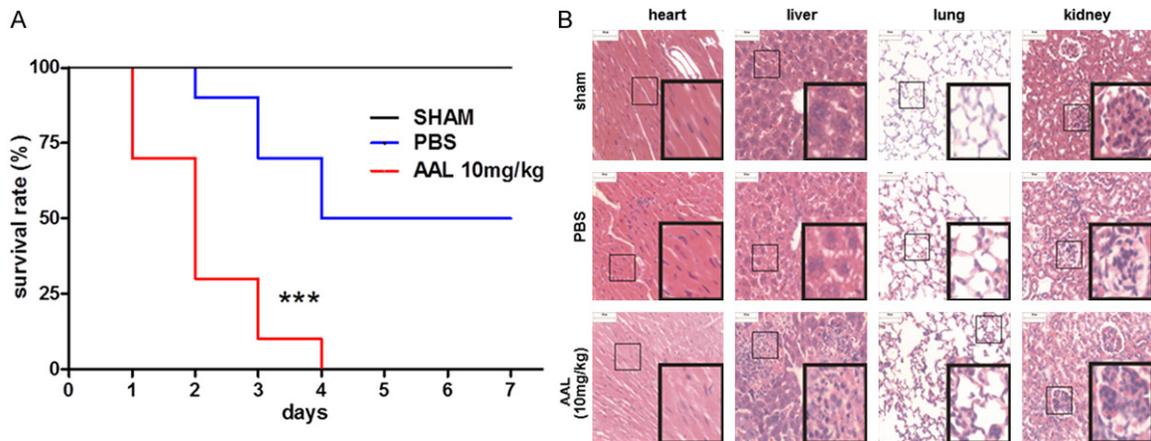
Figure 1. Survival rates and organ damages in CLP-induced septic shock. A. Administration of AAL exacerbated CLP-induced septic shock. Log-rank (Mantel-Cox) test was employed for data analysis. ***P < 0.001 as compared with the value in PBS treated micw. B. H&E staining analysis of heart, liver, lung and kidney sections derived from animals 48 h after CLP induction. Inset pictures were employed to show higher magnification of images for the indicated area.

described [14]. The isolated cells were washed twice in RPMI 1640 (HyClone, Logan, UT, USA) containing 10% FCS (HyClone, Logan, UT, USA), and then incubated at 4°C for 30 min with specific antibodies (PE-conjugated anti-F4/80, APC-conjugated anti-CD11b, Biolegend, San Diego, CA, USA; APC-conjugated anti-CD11c, FITC-conjugated anti-CD86, PE-conjugated anti-CD80, PE-conjugated anti-MHC-II, BD Biosciences San Jose, CA, USA), After washes the cells were analyzed using a FACSCalibur flow cytometer (BD Biosciences, San Jose, CA, USA) [15] and all data were analyzed using the FlowJo software (Tree Star Inc, Ashland, USA) as instructed.

Western blotting analysis

Culture supernatants were collected and mixed with a 1/10-fold volume of 100% trichloroacetic acid to precipitate proteins at -20°C for at least 30 min, and the precipitated proteins were washed once with 400µl cold acetone. Tissue or cells were homogenized in the RIPA lysis buffer (Beyotime, Shanghai, China) using a BBX24 Bullet Blender homogenizer (Next Advance Inc., Averill Park, NY, USA). Nuclear proteins (NE) were extracted using the NE-PER Nuclear and Cytoplasmic Extraction Reagents (Thermo Scientific, Lafayette, CO, USA). The prepared proteins were subjected to Western blotting with primary antibodies against Hmgb1 (Epitomics, California, USA), Dectin-1 (Thermo Scientific, MA, USA), RelA, Nlrp3 (R&D Systems, Minneapolis, MN, USA), di-/tri-methy H3K4,

p-Syk (Cell Signaling Technology, Danvers, MA, USA), p20, pro-Caspase-1, pro–IL-1β, Mincle, Syk, Card9, TLR2 and β-actin (Santa Cruz, CA, USA) as previously described [16].

Immunoprecipitation assay

Immunoprecipitation was performed using a Dynabeads® Protein G Immunoprecipitation Kit (Invitrogen, Carlsbad, USA) according to the manufacturer's instruction. Cellular extracts were first incubated with an Hmgb1 antibody (Epitomics, California, USA), and the protein complexes were then collected by using the Dynabeads. An anti-rabbit HRP-conjugated secondary antibody specific for IgG light chain (Boster, Wuhan, China) was used to avoid the detection of similar-sized IgG heavy chain on Western blots.

Confocal microscopy

Cells were plated and cultured overnight on glass slides. After fixation in 4% paraformaldehyde for 30 min and blocking with 10% FBS in PBS, the cells were permeabilized with Triton X-100 and incubated with an Hmgb1 antibody (Epitomics, California, USA). After incubation with an Alexa 594-conjugated secondary antibody (Invitrogen, Carlsbad, USA) for 1 h, the cells were further counterstained with DAPI (Invitrogen, Carlsbad, USA). Images were taken using a fluorescent confocal microscope (Carl Zeiss LSM 710) in scanning sequential mode and processed using the ZEN 2009 software (Carl Zeiss, Germany).
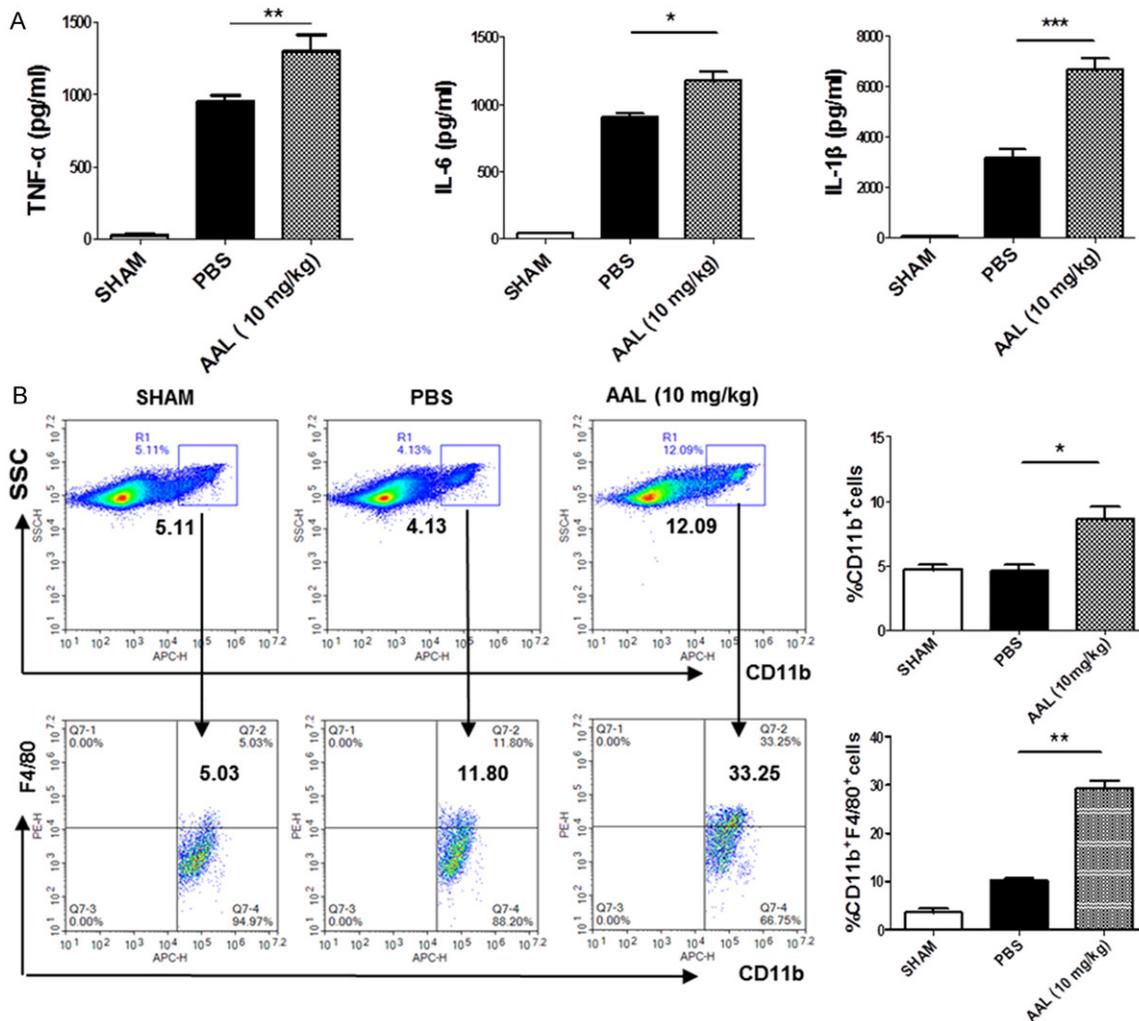
Figure 2. Serum cytokine levels in animals after CLP induction and the impact of AAL on macrophage recruitment. A. Serum levels for TNF-α, IL-6 and IL-1β 48 h after CLP induction. B. Flow cytometry analysis of splenic macrophages. Spleens were collected 48 h after CLP induction and then subjected to flow cytometry analysis. The cells were first gated for CD11b followed by analysis of F4/80+ cells. Left: a representative data for flow cytometry; right: a bar graphic figure showing the data with 5 replications. All data were expressed as mean ± SEM and analyzed by two-way ANOVA followed by Bonferroni test. *$P < 0.05$, **$P < 0.01$, ***$P < 0.001$ as compared with the values in PBS group.

RNA interference

Small-interfering RNA (siRNA) duplexes for silencing Mincle were designed using the RNAi Designer and synthesized by Ribobio (Guangzhou, Guangdong, China). The sequences for Mincle siRNA were as follows: siRNA: 5'-GCC GAU UGG UCU UCU GAAdTdT-3'. A scramble siRNA (5'-CUA CAA GAA CGC UGA AAUdTdT-3') was served as a control. siRNA Transfection was performed with Lipofectamine RNAi Max (Invitrogen, Carlsbad, USA) according to the established techniques [17].

Electrophoretic mobility shift assay (EMSA)

BMDM-derived nuclear proteins were employed for EMSA using the LightShift Chemiluminescent EMSA Kit (Thermo Scientific, Lafayette, CO, USA) and established techniques [17]. Biotin-labeled double-stranded oligonucleotides containing the NF-κB p65 binding site were used as a probe (forward: Biotin-5'-AGT TGA GGG GAC TTT CCC AGG C-3', reverse: Biotin-5'-GCC TGG GAA AGT CCC CTC AAC T-3'; Beyotime, Wuhan, China). A mixture of unlabeled probes was used as a negative control.
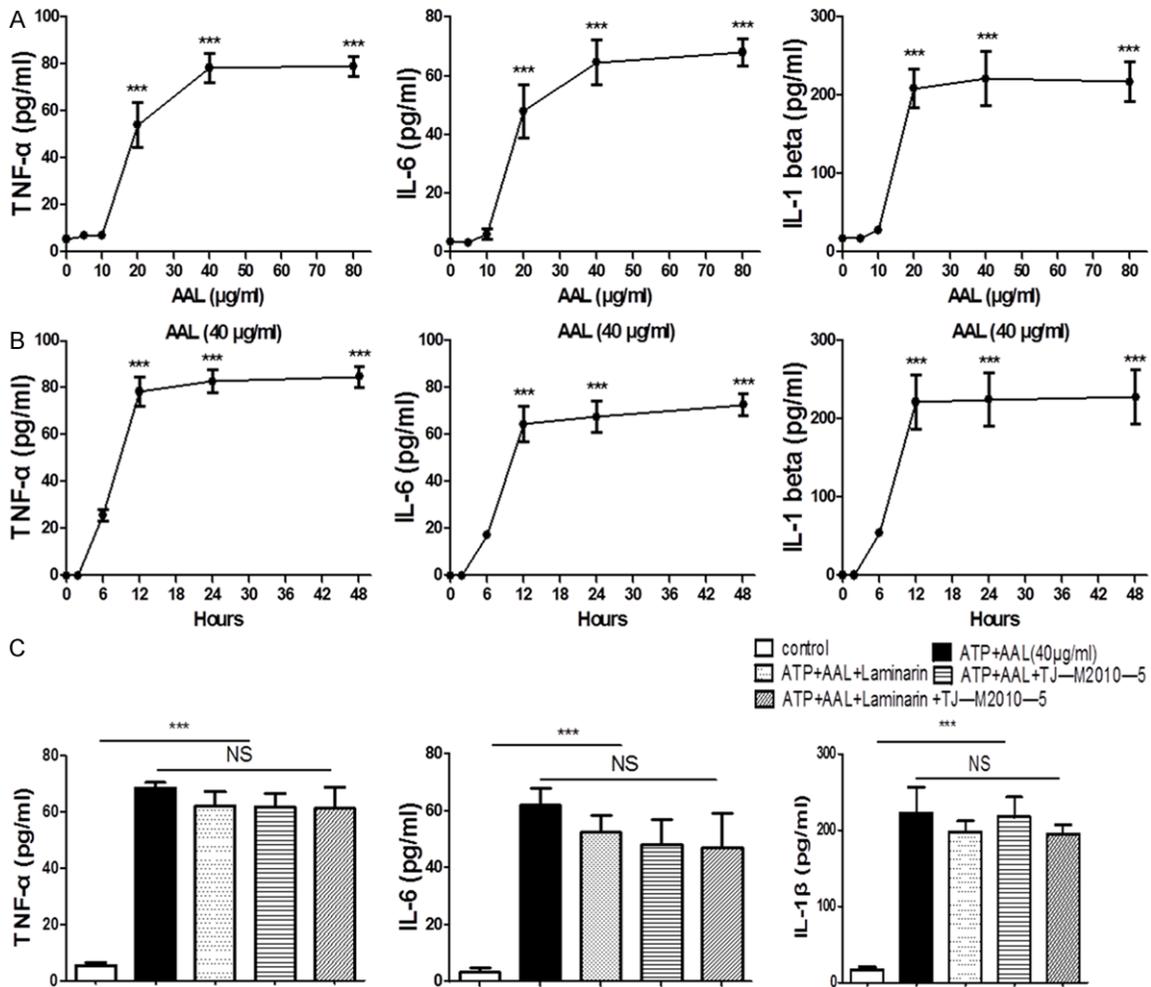
Figure 3. The impact of AAL stimulation on RAW264.7 cells. A. Analysis of optimal dose for AAL stimulation. RAW 264.7 cells were stimulated with different concentrations of AAL (0, 5, 10, 20, 40, 80 µg/ml) for 24 h, followed by analysis of TNF-α, IL-6 and IL-1β production. AAL at 40 µg/ml was noted to be the optimal concentration. B. Analysis of the optimal time for AAL stimulation. RAW 264.7 cells were stimulated with 40 µg/ml AAL for different time (0, 2, 6, 12, 24, 48 h), followed by analysis of TNF-α, IL-6 and IL-1β production. AAL stimulation for 12 h was noted to be the optimal time. C. Blockade of Dectin-1 and MyD88 did not affect AAL-induced cytokine secretion. RAW cells were pretreated for 30 min with Laminarin (100 µg/ml), an inhibitor for Dectin-1, and/or TJ-M2010-5 (10 µM), a blockade for MyD88, followed by AAL (40 µg/ml) stimulation for 12 h. ***$P < 0.001$ as compared with the values in the control group. Four samples were analyzed in each study group, and the data were analyzed by two-way ANOVA followed by Bonferroni test and expressed as mean ± SEM.

Data analysis

All experiments were carried out 3 times with replications, and the data were expressed as mean ± SEM. GraphPad Prism5 (GraphPad Software, San Diego, CA, USA) was employed for statistical analysis using Log-rank (Mantel-Cox) or one-way or two-way ANOVA as reported [18]. Bonferroni correction for post hoc *t* test was performed to compare the differences between groups when the first analysis revealed significant difference. *P* values less than 0.05 were considered statistically significant.

Results

AAL promotes the severity of CLP-induced sepsis

We first employed a CLP-induced septic shock model to assess the effect of AAL on pro-inflammatory responses. The dose for AAL administration was optimized as 10 mg/kg based on previous studies [8], and administration of 10 mg/kg AAL did not result in a perceptible side effect on normal mice but manifested a significant anti-tumor activity (data not
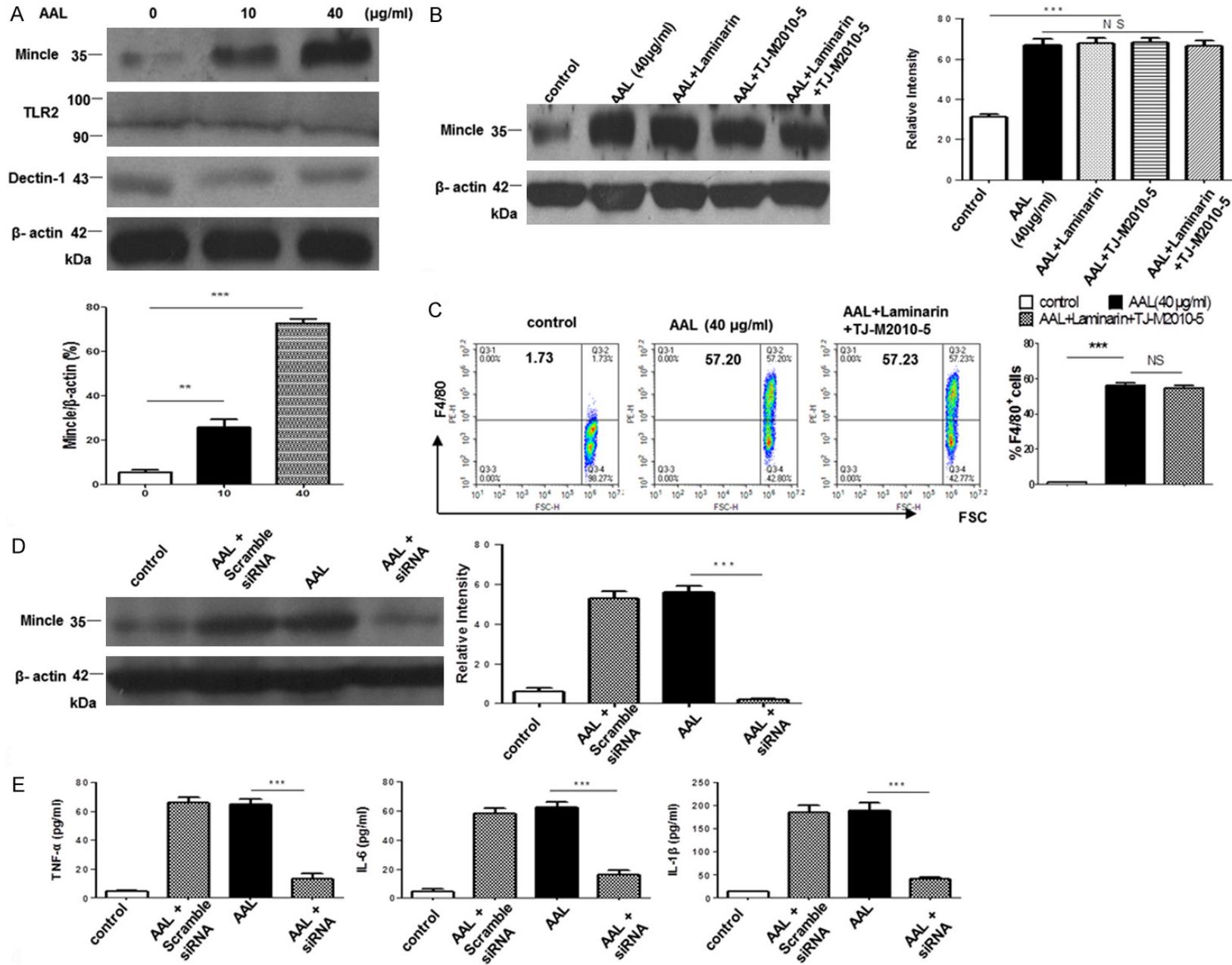
Figure 4. Mincle serves as a potential receptor for AAL signaling in macrophages. BMDMs were employed to characterize the potential receptor for AAL-63 signaling. A. AAL dose-dependently stimulated Mincle expression in BMDMs. Western blot analysis of AAL-stimulated BMDMs revealed that AAL preferentially stimulated BMDMs expression of high levels of Mincle. Upper: a representative Western blotting data; lower: a bar graphic figure showing the data with 4 replications. B. Blockade of Dectin-1 and TLR2 signaling did not attenuate AAL-induced Mincle expression. Addition of Laminarin and TJ-M2010-5 alone or in combination did not result in a significant change for AAL-induced Mincle expression. Left: a representative data for Western blot analysis; right: a bar graphic figure showing the data with 4 replications. C. Blockade of Dectin-1 and TLR2 signaling did not impact AAL-stimulated BMDM activation. BMDMs were stimulated with 40μg/ml AAL for 12 h in the presence of Laminarin and TJ-M2010-5 for 12 h, followed by flow cytometry analysis of F4/80$^+$ cells. Left: a representative flow cytometry data; right: a bar graphic figure showing the data with 4 replications. D. Transfection of a Mincle siRNA significantly repressed Mincle expression in BMDMs. Left: a representative Western blotting result; right: results with 4 replications. E. Knockdown of Mincle expression in BMDMs significantly attenuated AAL-induced production of TNF-α, IL-6 and IL-1β. The data were expressed as mean ± SEM and analyzed by two-way ANOVA followed by Bonferroni test, $**P < 0.01$, $***P < 0.001$ as compared with the values in the control group.

shown). As expected, administration of AAL significantly promoted CLP-induced lethality (**Figure 1A**). Consistently, much higher severity of pathological changes in the heart (cytolysis of the myocardium), liver (spotty necrotic scattering in the hepatic lobule), lung (hyperplasia of alveolar cells in the alveolar wall) and kidney (glomerular proliferation of glomerulus) was noted 48 h following CLP induction as compared with that of PBS treated mice (**Figure 1B**). Together, those data indicate that administration of AAL promotes the severity of CLP-induced sepsis.

AAL regulates macrophages secretion of inflammatory cytokines

We next examined the effect of AAL on inflammatory cytokine production in serum samples following 48 h CLP induction by ELISA. In consistent with the above observations, AAL treated mice manifested significantly higher levels of TNF-α, IL-6 and IL-1β as compared with that of PBS-treated control mice (**Figure 2A**). Since DCs and macrophages are sentinel cells to sense tissue/organ infection or injury and are responsible for the clearance of invaded pathogens, splenic cells 48 h after CLP induction were subjected to flow cytometry analysis to dissect the impact of AAL on the activity of DCs and macrophages. To our surprise, we failed to detect a significant difference for the number of DCs and their maturation states (CD80, CD86 and MHCII expressions) between AAL and PBS treated mice (Figure S1). However, AAL treatment not only increased the number of CD11b$^+$ monocytes but also promoted macrophage activation as manifested by the higher number of CD11b$^+$F4/80$^+$ macrophages as compared with that of control animals (**Figure 2B**). Collectively, our data suggest that AAL pro-

motes pro-inflammatory response by controlling the production of inflammatory cytokines, which involves the regulation of macrophage recruitment but not DCs.

Mincle serves as a potential receptor for AAL

We next sought to identify the receptor for AAL regulation of macrophage function, and an *in vitro* system was first established to resemble the effect of AAL in animals. RAW264.7 cells were stimulated with different concentration of AAL (0, 5, 10, 20, 40, 80 μg/ml), and the production of TNF-α, IL-1β and IL-6 was assayed at indicated time point. AAL failed to stimulate RAW264.7 cells secretion of these cytokines until its concentration reached 20 μg/ml, and the production of cytokines manifested a peak at 40 μg/ml AAL, while higher concentrations of AAL did not further increase cytokine secretion (**Figure 3A**). The highest levels for cytokines were detected once RAW264.7 cells stimulated with 40 μg/ml AAL for 12 h, and longer stimulation did not further significantly increase cytokine levels (**Figure 3B**). Therefore, AAL at 40 μg/ml with 12 h stimulation were selected for the following experiments.

The major C-type lectin receptors (CLRs) expressed on macrophages relevant to AAL are Dectin-1 and macrophage inducible C-type lectin (Mincle) [19, 20], we thus employed Laminarin, an inhibitor for Dectin-1, to block the potential signaling between AAL and Dectin-1. Other than Dectin-1 and Mincle, galectins are found capable of stimulating NF-κB and MAPK signaling in macrophages *via* TLR-2 [21]. Therefore, TJ-M2010-5, an inhibitor for TLR downstream molecule MyD88 [22], was also employed for the study. The above cells were cultured with AAL (40 μg/ml) in the presence of
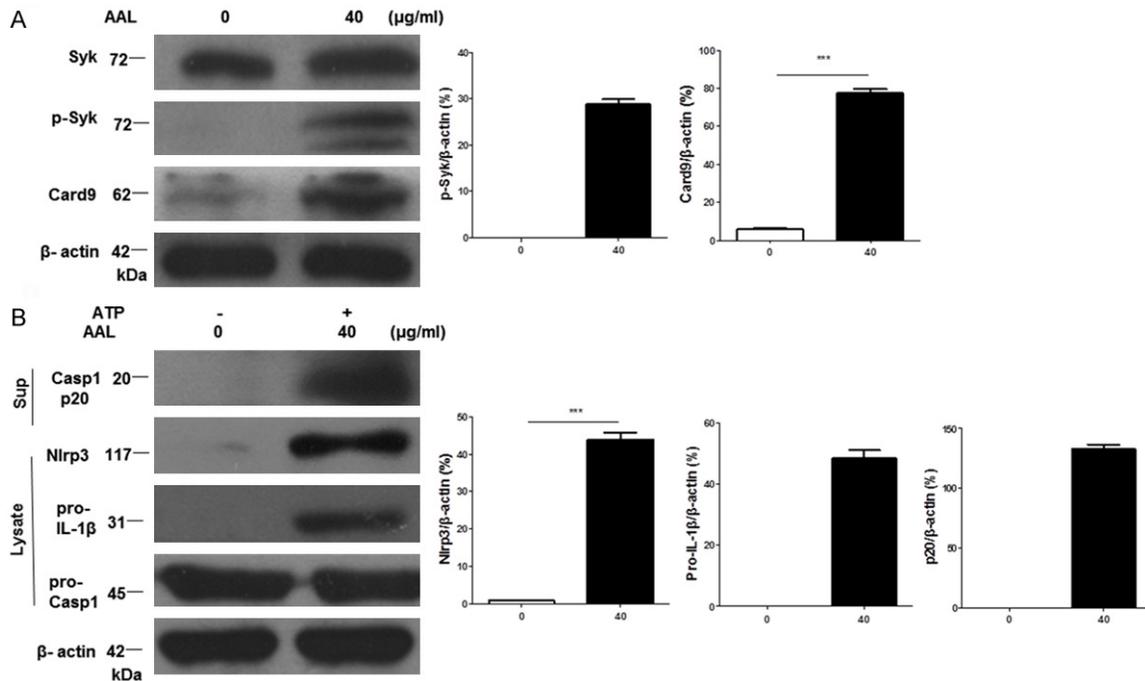
Figure 5. AAL activates Mincle/Syk/Card9 signaling to couple with Nlrp3 inflammasome assembly. The above pre-pared BMDM lysates were next subjected to Western blot analysis of Mincle down-stream molecules Syk and Card9 as well as Nlrp3 inflammasome assembly. A. Western blot analysis for the levels of Syk/Card9 signaling in AAL-stimulated BMDMs. Left: a representative Western blot result; right: results with 4 replications. B. Mincle/Syk/Card9 signaling couples to the Nlrp3 inflammasome assembly. Left: a representative result for Western blot analysis of Nlrp3, pro-IL-1β, pro-Casp1 and cleaved Casp1 (p20); right: Bar graphics figures showing the results with 4 replications. Four samples were analyzed in each study group, and the data were expressed as mean ± SEM and analyzed by two-way ANOVA, ***$P < 0.001$ compared with the value in control group.

Laminarin and/or TJ-M2010-5 as described. Interestingly, blockade of Dectin-1 and TLR signaling alone or both did not result in a perceptible impact on AAL stimulated cytokine secretion in RAW264.7 cells (**Figure 3C**). However, AAL dose-dependently increased Mincle expression, and in contrast, AAL did not stimulate a significant change for Dectin-1 and TLR-2 expression (**Figure 4A**). Particularly, addition of Laminarin and TJ-M2010-5 alone or in combination did not alter AAL induced Mincle expression (**Figure 4B**). Altogether, these data suggest that AAL regulates macrophages secretion of cytokines probably through receptor Mincle.

To further address the above question, bone-marrow derived macrophages (BMDMs) were pre-treated 12 h with AAL in the presence of Laminarin and/or TJ-M2010-5, followed by flow cytometry analysis of F4/80 expressions. AAL was found with high potency to stimulate BMDM activation as manifested by the significant increase of F4/80+ cells, irrespective the presence of Dectin-1 and/or TLR2 inhibitors (**Figure 4C**). Given that a Mincle specific blocker

is currently not available, a Mincle specific siRNA was then introduced into BMDMs, followed by AAL stimulation as above. As expected, siRNA significantly repressed AAL-induced Mincle expression as compared with that of scramble siRNA treated or untreated cells (**Figure 4D**). Remarkably, knockdown of Mincle expression significantly attenuated AAL-induced secretion of TNF-α, IL-1β and IL-6 (**Figure 4E**). Collectively, those data support that Mincle likely serves as a receptor for AAL-mediated effect on macrophages.

AAL-induced Mincle/Syk/Card9 signaling couples to the Nlrp3 inflammasome

Based on the above data, we then examined the impact of AAL on Mincle-mediated Syk/Card9 signaling. Western blot analysis revealed that AAL induced Syk activation as manifested by the increase of phosphorylated Syk (p-Syk) along with enhanced expression of Card9 in macrophages (**Figure 5A**). There is evidence that Syk signaling could couple to the Nlrp3 inflammasome [23, 24], we thus further exam-
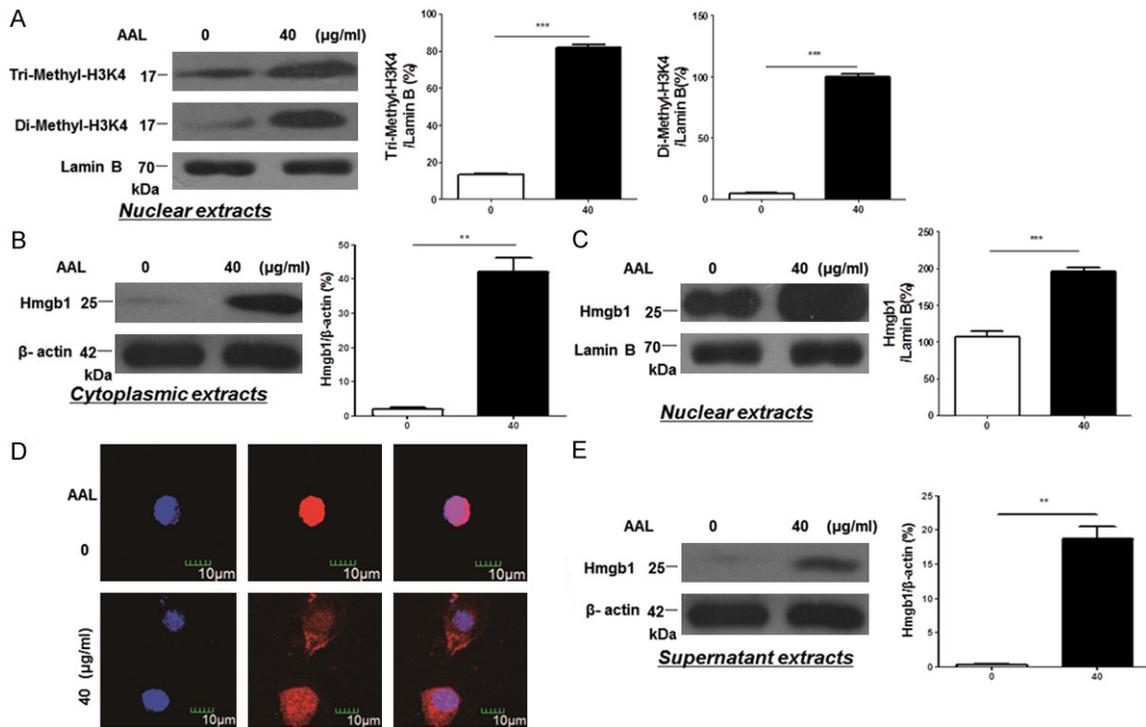
Figure 6. AAL modulates chromatin structure to regulate Hmgb1 secretion. A. AAL significantly stimulated H3K4 di-/ trimethylation in macrophages. Left: a representative result for Western blotting; right: bar graphic figures showing the data with 4 replications. B. Cytoplasmic Hmgb1 levels in macrophages following AAL stimulation. Left: a representative Western blot result; right: results with 4 replications. C. Nuclear Hmgb1 levels in macrophages following AAL stimulation. Left: a representative result for Western blotting; right: data obtained with 4 replications. D. Hmgb1 immunostaining in macrophages following AAL stimulation. AAL stimulated a significant Hmgb1 cytoplasmic translocation. E. Western blot analysis of Hmgb1 in AAL-stimulated macrophage culture supernatant. Left: a representative Western blot result; right: results with 4 replications. Four samples were analyzed in each study group, and the data were analyzed by two-way ANOVA followed by Bonferroni test and expressed as mean ± SEM. **$P < 0.01$, ***$P < 0.001$ compared with the value in control group.

ined Nlrp3 inflammasome assembly. Indeed, AAL induced high levels of Nlrp3 and pro-IL-1β expression (**Figure 5B**). In line with this result, high levels of cleaved Caspase 1 (Casp1, p20) were detected in the culture supernatants (**Figure 5B**). Since Nlrp3 inflammasome assembly would process the cleavage of pro-IL-1β, significant amount of IL-1β was detected in the supernatants (**Figure 3C**). Together, these data indicate that AAL activates Mincle/Syk/Card9 signaling which then couples to the Nlrp3 inflammasome to promote pro-inflammatory response in macrophages by regulating the secretion of inflammatory cytokines.

AAL modulates Hmgb1 function to regulate NFkB transcriptional activity

To further address the mechanisms by which AAL promotes cytokine secretion, we examined the impact of AAL on histone 3 (H3) methylation as chromatin signatures generated by epi-

genetic modification of histone proteins (e.g., methylation) play a crucial role for the control of gene expression [25, 26]. It was interestingly noted that AAL markedly promoted H3K4 di- and trimethylation (**Figure 6A**), which prompted us to embark on the high mobility group box protein 1 (Hmgb1), a well-known chromosomal protein associated with inflammatory response [27, 28]. Remarkably, AAL stimulation significantly increased Hmgb1 levels not only in the cytoplasm (**Figure 6B**) but also in the nucleus in macrophages (**Figure 6C**).

Based on the above observations, we first conducted Hmgb1 immunostaining of macrophages after AAL stimulation. Remarkably, AAL stimulated macrophages were characterized by the significant Hmgb1 cytoplasmic translocation (**Figure 6D**) along with active Hmgb1 secretion as manifested by the presence of high levels of Hmgb1 in the culture supernatants (**Figure 6E**). In line with these results, extracel-
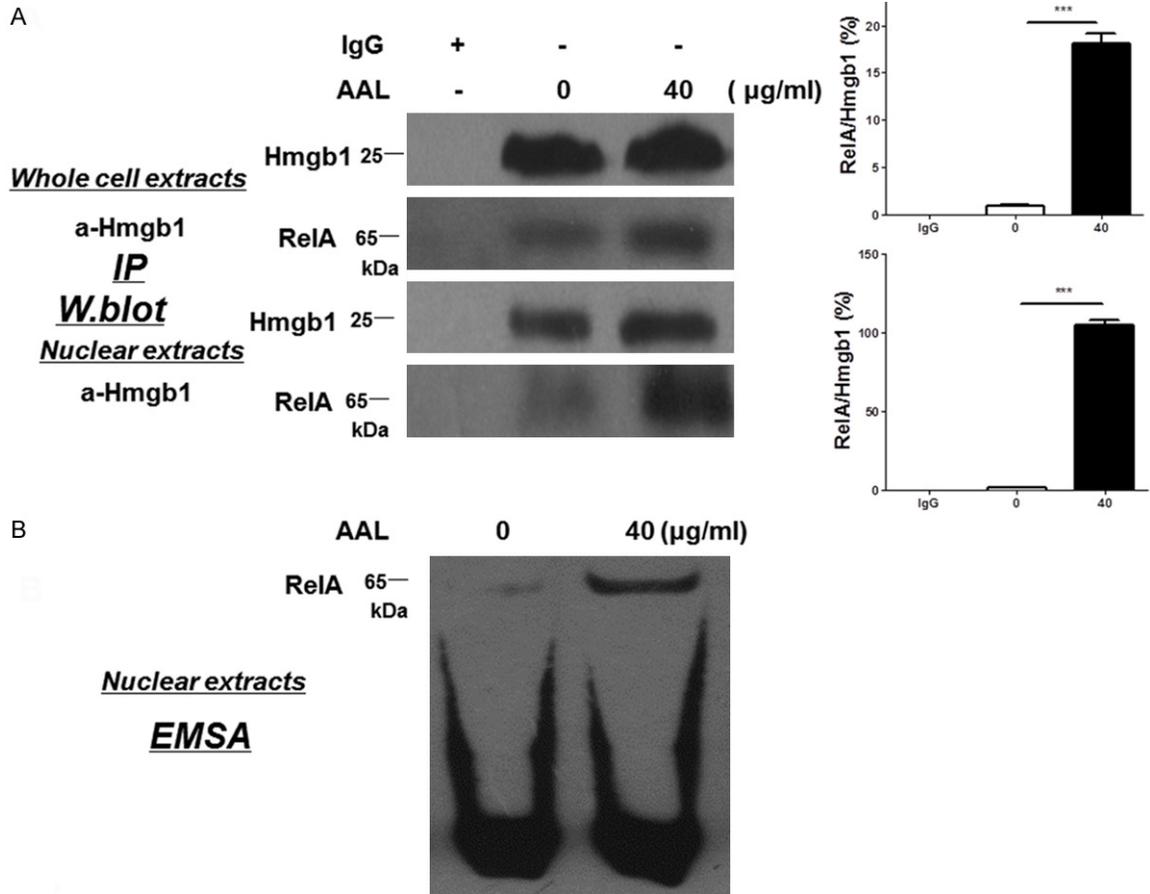
Figure 7. AAL induces nuclear Hmgb1 forming a complex with RelA to promote NFκB DNA binding activity. A. Western blot analysis of Hmgb1 immunoprecipitates. Upper panel: Hmgb1 immunoprecipitates resulted from AAL-stimulated whole macrophage extracts probed with antibodies against Hmgb1 and RelA, respectively. Lower panel: Hmgb1 immunoprecipitates originated from AAL-stimulated nuclear macrophage extracts probed with antibodies against Hmgb1 and RelA, respectively. Four samples were analyzed in each study group, and the data were expressed as mean ± SEM and analyzed by two-way ANOVA followed by Bonferroni test, ***P < 0.001 compared with the value in control group. B. EMSA results for analysis of NFκB DNA binding activity. The above prepared macrophage nuclear extracts were further employed for assessing NFκB DNA binding activity by EMSA.

lular Hmgb1 has been recognized to be a potent inflammatory mediator [29, 30]. To demonstrate the impact of AAL-induced nuclear Hmgb1 on inflammatory response, we conducted co-immunoprecipitation using an Hmgb1 antibody with AAL-stimulated whole cell extracts (WCE) and nuclear extracts (NE). It was interestingly found that RelA, a well-known NF-κB subunit essential for the transcription of inflammatory genes, was detected in the Hmgb1 precipitates (**Figure 7A**). Given that RelA levels were significantly higher in the precipitates originated from nuclear extracts as compared with that of whole cell extracts, and RelA was almost undetectable in the precipitates derived from unstimulated macrophages, those data suggest that AAL stimulates Hmgb1 expression and promotes Hmgb1 forming a complex with RelA in the nucleus. To confirm this notion, EMSA was employed to assess RelA DNA binding activity. Significantly higher DNA binding activity was noted in AAL stimulated macrophages as compared with that of unstimulated macrophages (**Figure 7B**). Taken all of those data together, our results suggest that AAL not only stimulates Hmgb1 secretion to exacerbate inflammatory response, but also promotes nuclear Hmgb1 forming a complex with RelA, and by which it modulates RelA DNA binding activity to enhance the transcription of inflammatory genes.

Discussion

It has been well recognized that fungi possess nutritional and medicinal virtue, and therefore,

many compounds bearing important pharmacological properties have been isolated from fungi such as polysaccharide-proteins and lectins [31]. In the current report we demonstrated evidence supporting that AAL, a galectin originated from edible mushrooms, possesses potent capacity to exacerbate pro-inflammatory response in the setting of CLP-induced sepsis. Of which, Mincle is likely serving as a potential receptor, and by which AAL activates Syk/Card9 signaling, which then couples to the Nlrp3 inflammasome. Particularly, AAL on the one hand stimulates macrophages secretion of copious amount of Hmgb1 to exacerbate pro-inflammatory response, it on the other hand promotes nuclear Hmgb1 to form a complex with NF-κB subunit RelA, and through which it enhances NF-κB DNA binding activity to promote the transcription of pro-inflammatory genes. Those studies provided novel insight into the understanding of mechanisms by which AAL stimulates pro-inflammatory response.

As an integral part of the innate immune system, DCs and macrophages are the primary sentinel cells to sense danger signals from infection and tissue or organ injuries by constantly sampling the environment [32]. Unexpectedly, we failed to obtain feasible evidence indicating a role for AAL in the regulation of DC recruitment or maturation. In contrast, AAL induced significantly higher ratio of CD11b$^+$ macrophages in the spleen along with enhanced activation as manifested by the higher number of CD11b$^+$F4/80$^+$ cells. These data suggest that AAL mediates pro-inflammatory response is likely by regulating the recruitment and activation of macrophages rather than DCs. Indeed, studies in bone marrow-derived DCs (BMDCs) further confirmed those data obtained in animals (data not shown).

Galectins, as galactoside-specific lectins, are associated with components for the extracellular matrix and counter receptors on the cell surface of mammalian cells [33]. Galectins are found to be implicated in a wide range of physiological processes such as apoptosis, inflammation, cell adhesion, and others [34]. Particularly, galectin AAL has been recognized with anti-tumor activity, while its specific receptor on macrophage surface is yet to be characterized. We optimized a culture system that resembles the conditions in animals. Given that blockade of Dectin-1 (by Laminarin) and TLR-2 (by TJ-M2010-5), the two receptors with possibility to interact with AAL, alone or in combination failed to attenuate the effect of AAL on macrophages, Mincle might serve as the receptor responsible for AAL signaling. Of note, we did not include a Mincle inhibitor for the current studies since its unavailability, and we also tried to obtain a Mincle knockout model but without success. We thus employed a Mincle siRNA and demonstrated that knockdown of Mincle expression significantly attenuated AAL-induced cytokine secretion, indicating that Mincle is likely to be the receptor for AAL signaling.

Mincle is one of the major receptors to recognize and bind lectin-like carbohydrates on leukocytes. Upon activation by binding to its cognate ligands, Mincle would mediate Syk phosphorylation, which then promotes Card9 signaling. In line with this notion, AAL induced Syk phosphorylation along with enhanced Card9 expression. Another interesting finding is that AAL activates Syk/Card9 signaling, which then couples to the Nlrp3 inflammasome. The Nlrp3 inflammasome is generally formed after oligomerization of Nlrp3 along with the recruitment of adaptor ASC (apoptosis-associated Speck-like protein with a caspase-recruitment domain) and pro-caspase-1 [35, 36], by which it generates cleaved caspase-1, which then processes the cleavage of pro-IL-1β and pro-IL-18 to produce mature IL-1β and IL-18 [37, 38]. Herein, these data support that AAL-induced Syk/Card9 signaling couples to the Nlrp3 inflammasome as manifested by the detection of enhanced Nlrp3 expression and cleaved Casp1 along with increased production of IL-1β.

It would be corollary to assume that the enhanced Syk/Card9 signaling along with the assembly of Nlrp3 inflammasome would activate NF-κB to promote inflammatory response. To dissect the underlying mechanisms, we checked the impact of AAL on chromatin structures. Interestingly, AAL promoted H3K4 di- and trimethylation, which is actually consistent with the well demonstrated concept that di/trimethylation of H3K4 is associated with the formation of euchromatin for gene transcription [39, 40]. To further get insight into the effect of chromatin structures on gene transcription, we examined the effect of AAL on the regulation of Hmgb1 functionality. As a non-specific DNA-binding architectural protein, Hmgb1 has been noted to regulate gene transcription by forming a complex with a particular transcription factor

[28]. However, Hmgb1 can also be passively released from damaged cells or actively secreted by innate immune cells such as macrophages [41, 42], and extracellular Hmgb1 acts as a potent inflammatory mediator to promote disease severity during the course of sepsis [43, 44]. Indeed, AAL induced significantly higher levels of Hmgb1 expression in macrophages. Particularly, AAL induced macrophages secretion of copious amount of Hmgb1 as manifested the Hmgb1 cytoplasmic translocation along with the detection of Hmgb1 in culture supernatant. AAL also stimulated a significant increase for nuclear Hmgb1, and analysis of nuclear Hmgb1 immunoprecipitates revealed that it formed a complex with RelA, and thereby enhancing NF-κB transcriptional activity as confirmed by EMSA analysis of DNA binding capacity. These results allowed us to conclude that AAL on the one hand stimulates macrophages secretion of large amount of Hmgb1 to exacerbate pro-inflammatory response; it on the other hand enhances the levels of nuclear Hmgb1, which then forms a complex with NF-κB subunit RelA to promote the transcription of pro-ifnlammatory responsive genes. Of note, the detailed mechanisms underlying the relationship between H3K4 methylation states and Hmgb1 subcellular location are yet to be fully addressed, which could involve additional epigenetic modifications such as acetylation, and therefore, additional studies would necessary to fully address this question.

In summary, we provided evidence that AAL exacerbates pro-inflammatory response in the setting of CLP-induced sepsis. AAL likely targets macrophages through the receptor Mincle to control the production of inflammatory cytokines by regulating Syk/Card9 signaling and Nlrp3 inflammasome assembly, which involve epigenetic modification of chromatin structure along with the regulation of Hmgb1 functionality. These data suggest that AAL regulates immune response by specifically targeting macrophages *via* receptor Mincle, which may possess important pharmaceutical properties in clinical settings.

Acknowledgements

Declaration of conflict of interest

None.

Address correspondence to: Dr. Cong-Yi Wang, The Center for Biomedical Research, Tongji Hospital, Wuhan, China. Tel: 86-27-8366-3485; E-mail: wang-cy@tjh.tjmu.edu.cn; Dr. Hui Sun, College of Life Science, Wuhan University, Wuhan China Tel: 86-27-6875-4027; E-mail: sunhui@whu.edu.cn

References

[1] Hagemann T, Lawrence T, McNeish I, Charles KA, Kulbe H, Thompson RG, Robinson SC and Balkwill FR. "Re-educating" tumor-associated macrophages by targeting NF-kappaB. J Exp Med 2008; 205: 1261-1268.

[2] Gaurnier-Hausser A, Rothman VL, Dimitrov S and Tuszynski GP. The novel angiogenic inhibitor, angiocidin, induces differentiation of monocytes to macrophages. Cancer Res 2008; 68: 5905-5914.

[3] Wajant H, Pfizenmaier K and Scheurich P. Tumor necrosis factor signaling. Cell Death Differ 2003; 10: 45-65.

[4] Fridman WH, Pages F, Sautes-Fridman C and Galon J. The immune contexture in human tumours: impact on clinical outcome. Nat Rev Cancer 2012; 12: 298-306.

[5] Sica A, Larghi P, Mancino A, Rubino L, Porta C, Totaro MG, Rimoldi M, Biswas SK, Allavena P and Mantovani A. Macrophage polarization in tumour progression. Semin Cancer Biol 2008; 18: 349-355.

[6] Sica A and Mantovani A. Macrophage plasticity and polarization: in vivo veritas. J Clin Invest 2012; 122: 787-795.

[7] Liang Y, Lin JC, Wang K, Chen YJ, Liu HH, Luan R, Jiang S, Che T, Zhao Y, Li de F, Wang da C, Guo L and Sun H. A nuclear ligand MRG15 involved in the proapoptotic activity of medicinal fungal galectin AAL (Agrocybe aegerita lectin). Biochim Biophys Acta 2010; 1800: 474-480.

[8] Zhao C, Sun H, Tong X and Qi Y. An antitumour lectin from the edible mushroom Agrocybe aegerita. Biochem J 2003; 374: 321-327.

[9] Yang N, Li DF, Feng L, Xiang Y, Liu W, Sun H and Wang DC. Structural basis for the tumor cell apoptosis-inducing activity of an antitumor lectin from the edible mushroom Agrocybe aegerita. J Mol Biol 2009; 387: 694-705.

[10] Han J, Zhong J, Wei W, Wang Y, Huang Y, Yang P, Purohit S, Dong Z, Wang MH, She JX, Gong F, Stern DM and Wang CY. Extracellular high-mobility group box 1 acts as an innate immune mediator to enhance autoimmune progression and diabetes onset in NOD mice. Diabetes 2008; 57: 2118-2127.

[11] Zhong J, Yu Q, Yang P, Rao X, He L, Fang J, Tu Y, Zhang Z, Lai Q, Zhang S, Kuczma M, Kraj P, Xu JF, Gong F, Zhou J, Wen L, Eizirik DL, Du J, Wang W and Wang CY. MBD2 regulates TH17 differentiation and experimental autoimmune encephalomyelitis by controlling the homeostasis of T-bet/Hlx axis. J Autoimmun 2014; 53: 95-104.

[12] Zou R, He Y, Li YQ, Han M, Ma ZF, Liu XC, Zeng R, Shao JF, Guo YC, He XY, Yang P, Xu G, Wang CY and Yao Y. Telmisartan protects 5/6 Nx rats against renal injury by enhancing nNOS-derived NO generation via regulation of PPARgamma signaling. Am J Transl Res 2014; 6: 517-527.

[13] Zeng JC, Lin DZ, Yi LL, Liu GB, Zhang H, Wang WD, Zhang JA, Wu XJ, Xiang WY, Kong B, Chen ZW, Wang CY and Xu JF. BTLA exhibits immune memory for alphabeta T cells in patients with active pulmonary tuberculosis. Am J Transl Res 2014; 6: 494-506.

[14] Fang J, He L, Wang SQ, Ma MJ, Liu HY, Zhu XH, Zhu P, Wei X and Wang CY. A simplified two-stitch sleeve technique for arterial anastomosis of cervical heterotopic cardiac transplantation in mice. Am J Transl Res 2013; 5: 521-529.

[15] Chen XQ, Liu XF, Liu WH, Guo W, Yu Q and Wang CY. Comparative analysis of dendritic cell numbers and subsets between smoking and control subjects in the peripheral blood. Int J Clin Exp Pathol 2013; 6: 290-296.

[16] Yang P, Zhang Y, Pang J, Zhang S, Yu Q, He L, Wagner KU, Zhou Z and Wang CY. Loss of Jak2 impairs endothelial function by attenuating Raf-1/MEK1/Sp-1 signaling along with altered eNOS activities. Am J Pathol 2013; 183: 617-625.

[17] Rao X, Zhong J, Zhang S, Zhang Y, Yu Q, Yang P, Wang MH, Fulton DJ, Shi H, Dong Z, Wang D and Wang CY. Loss of methyl-CpG-binding domain protein 2 enhances endothelial angiogenesis and protects mice against hind-limb ischemic injury. Circulation 2011; 123: 2964-2974.

[18] Tu Y, Yu Q, Fan G, Yang P, Lai Q, Yang F, Zhang S, Wang W, Wang D, Yu X and Wang CY. Assessment of type 2 diabetes risk conferred by SNPs rs2241766 and rs1501299 in the ADIPOQ gene, a case/control study combined with meta-analyses. Mol Cell Endocrinol 2014; 396: 1-9.

[19] Veldhuizen EJ, van Eijk M and Haagsman HP. The carbohydrate recognition domain of collectins. FEBS J 2011; 278: 3930-3941.

[20] Kanazawa N, Tashiro K and Miyachi Y. Signaling and immune regulatory role of the dendritic cell immunoreceptor (DCIR) family lectins: DCIR, DCAR, dectin-2 and BDCA-2. Immunobiology 2004; 209: 179-190.

[21] Kammanadiminti SJ, Mann BJ, Dutil L and Chadee K. Regulation of Toll-like receptor-2 expression by the Gal-lectin of Entamoeba histolytica. FASEB J 2004; 18: 155-157.

[22] Li C, Huang X, Liu Y, Yang T, Zhang L, Li M, Jiang F, Huang W and Zhou P. Dendritic cells play an essential role in transplantation responses via myeloid differentiation factor 88 signaling. Transplant Proc 2013; 45: 1842-1845.

[23] Yasukawa S, Miyazaki Y, Yoshii C, Nakaya M, Ozaki N, Toda S, Kuroda E, Ishibashi K, Yasuda T, Natsuaki Y, Mi-ichi F, Iizasa E, Nakahara T, Yamazaki M, Kabashima K, Iwakura Y, Takai T, Saito T, Kurosaki T, Malissen B, Ohno N, Furue M, Yoshida H and Hara H. An ITAM-Syk-CARD9 signalling axis triggers contact hypersensitivity by stimulating IL-1 production in dendritic cells. Nat Commun 2014; 5: 3755.

[24] Kistowska M, Fenini G, Jankovic D, Feldmeyer L, Kerl K, Bosshard P, Contassot E and French LE. Malassezia yeasts activate the NLRP3 inflammasome in antigen-presenting cells via Syk-kinase signalling. Exp Dermatol 2014; 23: 884-889.

[25] Alderton GK. Epigenetics: Histone methylation: it's in the numbers. Nat Rev Cancer 2014; 15: 1.

[26] Sekar TV, Foygel K, Gelovani JG and Paulmurugan R. Genetically encoded molecular biosensors to image histone methylation in living animals. Anal Chem 2015; 87: 892-9.

[27] Wang H, Liao H, Ochani M, Justiniani M, Lin X, Yang L, Al-Abed Y, Wang H, Metz C, Miller EJ, Tracey KJ and Ulloa L. Cholinergic agonists inhibit HMGB1 release and improve survival in experimental sepsis. Nat Med 2004; 10: 1216-1221.

[28] El Gazzar M, Yoza BK, Chen X, Garcia BA, Young NL and McCall CE. Chromatin-specific remodeling by HMGB1 and linker histone H1 silences proinflammatory genes during endotoxin tolerance. Mol Cell Biol 2009; 29: 1959-1971.

[29] Muller S, Scaffidi P, Degryse B, Bonaldi T, Ronfani L, Agresti A, Beltrame M and Bianchi ME. New EMBO members' review: the double life of HMGB1 chromatin protein: architectural factor and extracellular signal. EMBO J 2001; 20: 4337-4340.

[30] Thomas JO and Travers AA. HMG1 and 2, and related 'architectural' DNA-binding proteins. Trends Biochem Sci 2001; 26: 167-174.

[31] Wang HX, Liu WK, Ng TB, Ooi VE and Chang ST. The immunomodulatory and antitumor activities of lectins from the mushroom Tricholoma

mongolicum. Immunopharmacology 1996; 31: 205-211.

[32] Zhang S, Zhong J, Yang P, Gong F and Wang CY. HMGB1, an innate alarmin, in the pathogenesis of type 1 diabetes. Int J Clin Exp Pathol 2009; 3: 24-38.

[33] Takeuchi T, Tamura M, Nishiyama K, Iwaki J, Hirabayashi J, Takahashi H, Natsugari H, Arata Y and Kasai K. Mammalian galectins bind galactosebeta1-4fucose disaccharide, a unique structural component of protostomial N-type glycoproteins. Biochem Biophys Res Commun 2013; 436: 509-513.

[34] Wang HX, Ng TB and Ooi VE. A protein with inhibitory activity on cell-free translation from cultured mycelia of the edible mushroom Tricholoma lobayense. Comp Biochem Physiol B Biochem Mol Biol 2000; 125: 247-253.

[35] Latz E, Xiao TS and Stutz A. Activation and regulation of the inflammasomes. Nat Rev Immunol 2013; 13: 397-411.

[36] Baroja-Mazo A, Martin-Sanchez F, Gomez AI, Martinez CM, Amores-Iniesta J, Compan V, Barbera-Cremades M, Yague J, Ruiz-Ortiz E, Anton J, Bujan S, Couillin I, Brough D, Arostegui JI and Pelegrin P. The NLRP3 inflammasome is released as a particulate danger signal that amplifies the inflammatory response. Nat Immunol 2014; 15: 738-748.

[37] Pedra JH, Cassel SL and Sutterwala FS. Sensing pathogens and danger signals by the inflammasome. Curr Opin Immunol 2009; 21: 10-16.

[38] Zhou R, Yazdi AS, Menu P and Tschopp J. A role for mitochondria in NLRP3 inflammasome activation. Nature 2011; 469: 221-225.

[39] Chaturvedi CP, Somasundaram B, Singh K, Carpenedo RL, Stanford WL, Dilworth FJ and Brand M. Maintenance of gene silencing by the coordinate action of the H3K9 methyltransferase G9a/KMT1C and the H3K4 demethylase Jarid1a/KDM5A. Proc Natl Acad Sci U S A 2012; 109: 18845-18850.

[40] Du Z, Li H, Wei Q, Zhao X, Wang C, Zhu Q, Yi X, Xu W, Liu XS, Jin W and Su Z. Genome-wide analysis of histone modifications: H3K4me2, H3K4me3, H3K9ac, and H3K27ac in Oryza sativa L. Japonica. Mol Plant 2013; 6: 1463-1472.

[41] Qin S, Wang H, Yuan R, Li H, Ochani M, Ochani K, Rosas-Ballina M, Czura CJ, Huston JM, Miller E, Lin X, Sherry B, Kumar A, Larosa G, Newman W, Tracey KJ and Yang H. Role of HMGB1 in apoptosis-mediated sepsis lethality. J Exp Med 2006; 203: 1637-1642.

[42] Huang Y, Yin H, Han J, Huang B, Xu J, Zheng F, Tan Z, Fang M, Rui L, Chen D, Wang S, Zheng X, Wang CY and Gong F. Extracellular hmgb1 functions as an innate immune-mediator implicated in murine cardiac allograft acute rejection. Am J Transplant 2007; 7: 799-808.

[43] Yang L, Xie M, Yang M, Yu Y, Zhu S, Hou W, Kang R, Lotze MT, Billiar TR, Wang H, Cao L and Tang D. PKM2 regulates the Warburg effect and promotes HMGB1 release in sepsis. Nat Commun 2014; 5: 4436.

[44] Wang H, Yang H and Tracey KJ. Extracellular role of HMGB1 in inflammation and sepsis. J Intern Med 2004; 255: 320-331.

Immunosuppression of AAL by mincle
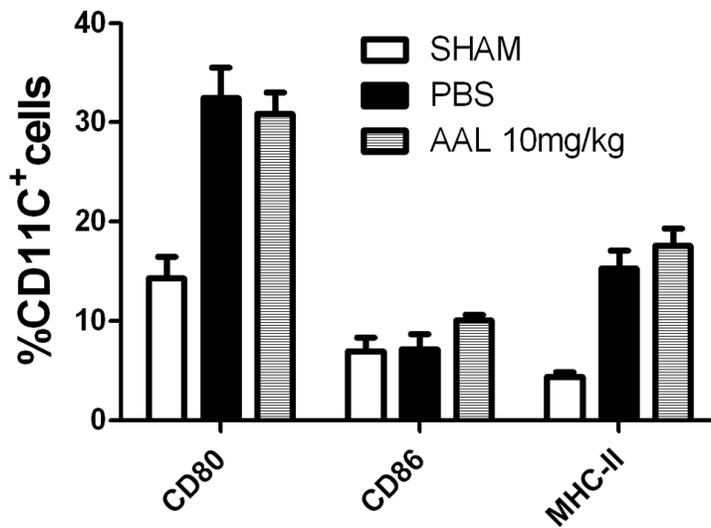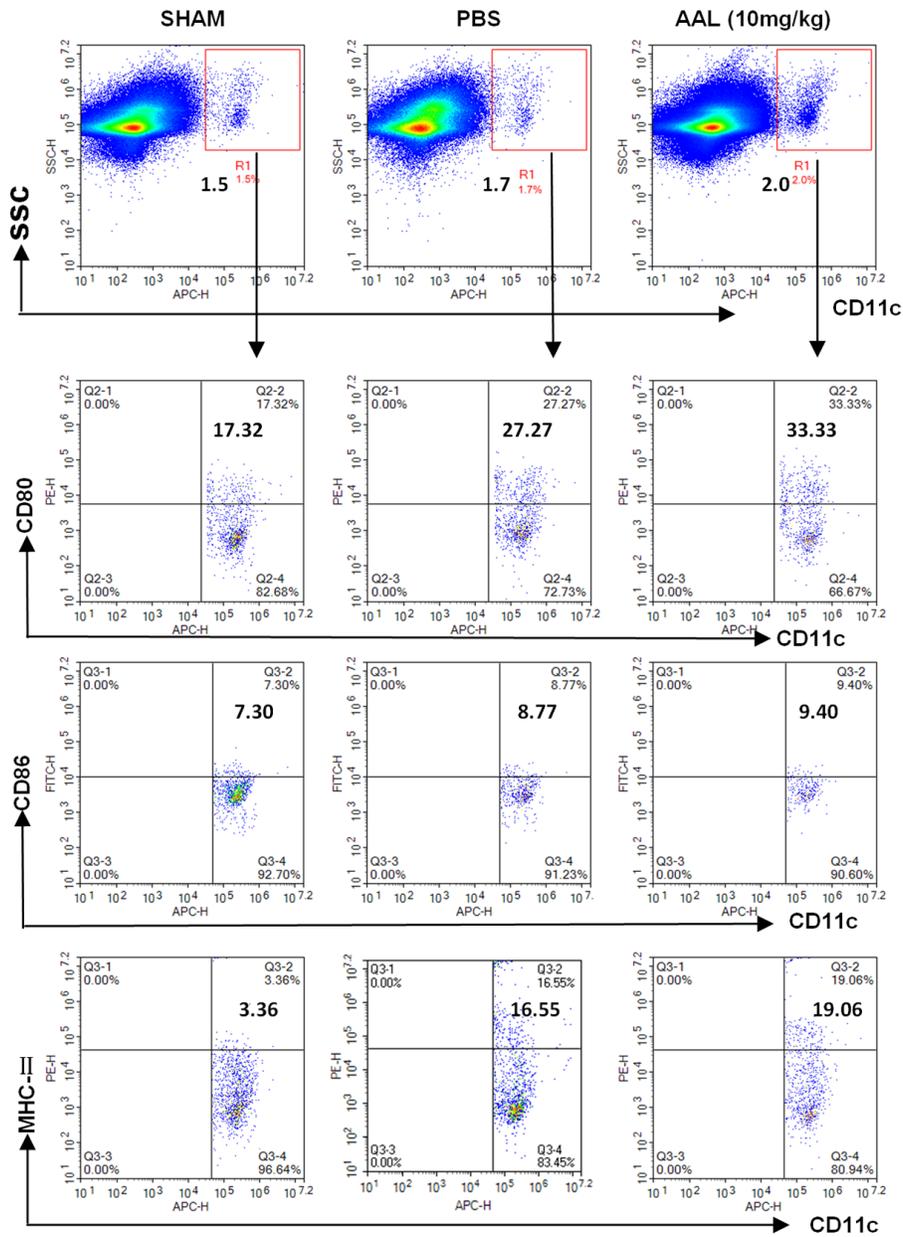
Figure S1. Flow cytometry analysis for the ratio of splenic DCs in three-group mice 48 h after CLP (n = 5 for each group).